Glutamate receptor dynamics organizing synapse formation in vivo

Article *in* Nature Neuroscience · August 2005

DOI: 10.1038/nn1484 · Source: PubMed

14 authors, including:

Wernher Fouquet
Leica Microsystems
22 PUBLICATIONS **2,175** CITATIONS

SEE PROFILE

Robert J Kittel
University of Leipzig
60 PUBLICATIONS **3,422** CITATIONS

SEE PROFILE

Sara Mertel
Freie Universität Berlin
34 PUBLICATIONS **2,071** CITATIONS

SEE PROFILE

nature neuroscience

Glutamate receptor dynamics organizing synapse formation *in vivo*

Tobias M Rasse[1], Wernher Fouquet[1], Andreas Schmid[1], Robert J Kittel[1], Sara Mertel[1], Carola B Sigrist[1], Manuela Schmidt[1], Asja Guzman[1], Carlos Merino[1], Gang Qin[1], Christine Quentin[1], Frank F Madeo[2], Manfred Heckmann[3] & Stephan J Sigrist[1]

Insight into how glutamatergic synapses form *in vivo* is important for understanding developmental and experience-triggered changes of excitatory circuits. Here, we imaged postsynaptic densities (PSDs) expressing a functional, GFP-tagged glutamate receptor subunit (GluR-IIA^{GFP}) at neuromuscular junctions of *Drosophila melanogaster* larvae for several days *in vivo*. New PSDs, associated with functional and structural presynaptic markers, formed independently of existing synapses and grew continuously until reaching a stable size within hours. Both *in vivo* photoactivation and photobleaching experiments showed that extrasynaptic receptors derived from diffuse, cell-wide pools preferentially entered growing PSDs. After entering PSDs, receptors were largely immobilized. In comparison, other postsynaptic proteins tested (PSD-95, NCAM and PAK homologs) exchanged faster and with no apparent preference for growing synapses. We show here that new glutamatergic synapses form *de novo* and not by partitioning processes from existing synapses, suggesting that the site-specific entry of particular glutamate receptor complexes directly controls the assembly of individual PSDs.

Glutamate receptors localized within the PSD region transmit the excitatory responses in the brain and in many other neuronal systems. Thus, a detailed molecular and cell-biological insight into the formation of glutamatergic synapses is important for our understanding of the development of excitatory neuronal circuits and for long-term information storage in the CNS[1]. So far, formation of glutamatergic synapses has been studied mainly in cultivated brain neurons. These studies have been helpful, for example, in delineating a temporal sequence of pre- and postsynaptic assembly and characterizing mechanisms of glutamate receptor trafficking during synapse formation[2–4].

How glutamatergic synapses assemble *in vivo* remains to be addressed. It is conceivable that synapse formation is more tightly controlled temporally and spatially *in vivo* than *in vitro*, particularly when synapses are added to strengthen already functional circuits[5]. It is thus important to follow 'the entire history' of identified synapses over time in the intact organism while monitoring their molecular dynamics and functional features. Analysis of synapse formation *in vivo* might profit from the use of synaptic models that are optically and genetically highly accessible. The Drosophila neuromuscular junction (NMJ) is a well established glutamatergic model, widely used for functional genetic descriptions of principle glutamatergic transmission. A mature NMJ comprises a few hundred individual synapses, which are ultrastructurally similar to central mammalian synapses[6,7] and express glutamate receptor subunits (GluR-IIA, GluR-IIB, GluR-IIC, GluR-IID, GluR-IIE) related to mammalian non-NMDA type glutamate receptors[8–11]. NMJs comprised of motor neurons and somatic muscles form during late embryonic development in Drosophila. The number of individual synaptic sites per NMJ increases throughout subsequent larval development[12]. Thus, the NMJ should be a suitable model for studying the new formation of glutamatergic synapses within a functional circuit.

Here, we have imaged functional, GFP-labeled glutamate receptors (GluR-IIA^{GFP}) during the formation of new NMJ synapses *in vivo*. We show that new small receptor fields form *de novo* and not by discrete partitioning events. These new small receptor fields correspond to the PSD region of functional synapses, as they are tightly associated with both independent PSD markers and functional (styryl dye labeling) and molecular (active zone components, calcium channels) markers of presynaptic active sites. Small PSDs grow for many hours before finally stabilizing at a mature size. Fluorescence recovery after photobleaching (FRAP) and photoactivation experiments indicate that the incorporation of GluR-IIA-containing glutamate receptor complexes from extrasynaptic pools is directly instructive for PSD formation and growth and, as a result, synapse formation.

RESULTS

In vivo labeling of individual PSDs at NMJs of Drosophila

We aimed to investigate in fully native settings how glutamatergic synapses form and how glutamate receptor dynamics are organized during this process. The transparent nature of Drosophila larvae make

[1]European Neuroscience Institute Göttingen, Max-Planck-Society, Waldweg 33, D-37073 Göttingen, Germany. [2]IMB, Universitätsplatz 2, Karl Franzens Universität, Graz, Austria. [3]Physiologisches Institut, Hermann-Herder-Str. 7, D-79104 Freiburg, Germany. Correspondence should be addressed to S.J.S. (ssigris@gwdg.de) and M.H. (heckmann@physiologie.uni-freiburg.de).

Published online 26 June 2005; doi:10.1038/nn1484

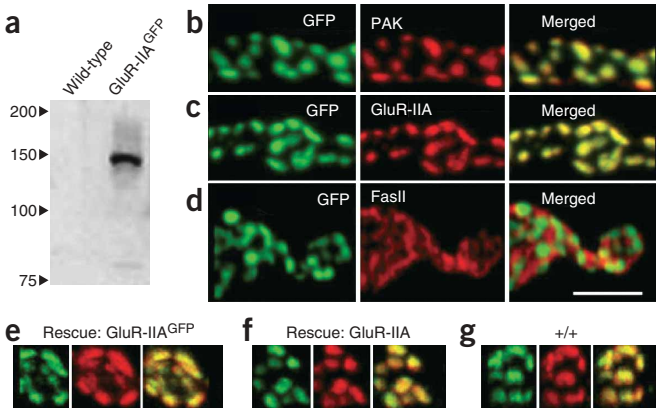

Figure 1 GluR-IIA^{GFP} labels the PSDs of individual NMJ synapses. (**a**) Western blot analysis in which antibodies to GFP were used to probe extracts of embryos transgenically expressing GluR-IIA^{GFP}. Wild-type embryos were used as controls. (**b**–**g**) Confocal images of immunofluorescent staining showing NMJ 6/7 of mid–third instar Drosophila larvae. (**b**–**d**) Larva expressing one transgene copy of GluR-IIA^{GFP} (GluR-IIA^{GFP}/+) stained for GFP (**b**–**d**), PAK (**b**), GluR-IIA (**c**) or FasII (**d**). Merged images are shown at right. Scale bar, 3 μm. (**e**,**f**) *GluRIIA* and *GluRIIB* double-mutant larvae (see Methods) rescued by GluR-IIA^{GFP} (**e**) or untagged GluR-IIA (**f**) expression, stained for GluR-IIA (green) and GluR-IIC (red). (**g**) Wild-type control larva stained for GluR-IIA (green) and GluR-IIC (red).

them an ideal subject in which to examine the glutamatergic synapses forming at the developing larval NMJ. To label glutamate receptors for *in vivo* imaging, we inserted enhanced GFP (EGFP) into the middle of the intracellular C terminus of GluR-IIA[13]. We then expressed GluR-IIA^{GFP} from a genomic transgene[9]. In western blots probed with antibodies to GFP (**Fig. 1a**), we detected GluR-IIA^{GFP} at the predicted 140 kDa in extracts of GluR-IIA^{GFP} transgenic embryos. Next, we evaluated the subcellular distribution of GluR-IIA^{GFP} by immunofluorescent staining of Drosophila NMJs. In such stainings, GluR-IIA is known to label individual PSDs[8]. Likewise, GluR-IIA^{GFP} expression was confined to individual PSDs. We found that GluR-IIA^{GFP} strictly colocalized with p21/rac1-activated kinase (PAK), an established PSD marker[14,15], and with endogenous GluR-IIA (**Fig. 1b**,**c**). Furthermore, GluR-IIA^{GFP} patches were surrounded (**Fig. 1d**) by the typical perisynaptic expression of the neural cell adhesion molecule (NCAM) homolog fasciclin II (FasII)[15]. In the *GluRIIA* and *GluRIIB* double-mutant background, the transgenic expression of GluR-IIA mediated by either GluR-IIA^{GFP} (**Fig. 1e**) or GluR-IIA (**Fig. 1f**) was indistinguishable, and it was similar to the level of GluR-IIA expression found at wild-type NMJs (**Fig. 1g**). Also, GluR-IIA and GluR-IIA^{GFP} colocalized with GluR-IIC (**Fig. 1e–g**). The GluR-IIC subunit is essential for NMJ neurotransmission, probably by acting as an obligate binding partner of GluR-IIA for forming functional channels[10]. In short, GluR-IIA^{GFP} was expressed at physiological levels, and individual receptor fields corresponded to individual PSDs. From this point on, receptor fields identified by means of GluR-IIA^{GFP} will be referred to as PSDs.

Finally, we characterized GluR-IIA^{GFP} in functional terms. Consistent with GluR-IIA^{GFP} being fully functional, we found that GFP-labeled GluR-IIA rescued *GluRIIA* and *GluRIIB*-deficient animals, giving rise to viable adults in a mendelian ratio. To directly assess the functionality of GluR-IIA^{GFP}, we carried out two-electrode voltage-clamp recordings on third instar larvae. Evoked and spontaneous NMJ currents were indistinguishable between GFP-labeled and wild-type GluR-IIA rescued animals (**Fig. 2**). Thus, we found that the function and intracellular distribution of GluR-IIA^{GFP} is identical to that of unlabeled wild-type GluR-IIA. Thus, GluR-IIA^{GFP} is a suitable tool to track the development of individual PSDs, as well as glutamate receptor dynamics during this process, *in vivo*.

New PSDs form at sites distant from existing synapses

We next sought to observe the formation of additional PSDs by imaging GluR-IIA^{GFP} at identified developing NMJs *in vivo*. As shown previously[16], we found that the overall morphology of an individual NMJ is relatively stable during larval development, but its size increases substantially (**Fig. 3a**). The morphological size, functional strength[17] and the number of individual synaptic sites per NMJ[12] are all known to increase during larval development. Consistently, we observed that many new PSDs formed at locations more or less equally distributed over the NMJ during development, mostly at sites distant from existing PSDs (**Fig. 3b**, arrows). To quantify formation and growth of individual PSDs, we pooled data from five experiments. In this data set, synapses were followed in 12-h intervals over 36 h at 16 °C (corresponding to about 12 h of development at 25 °C; unpublished data). This time window represents about 20% of larval development. In this time interval, we observed a 53% increase in PSD number (starting with 309 individual PSDs, we observed the formation of 165 new PSDs). At the same time, the overall size distribution of PSDs seemed rather stable (**Fig. 3c**) and the mean PSD size increased by only 14% within these 36 h (from 0.21 μm^2 at 0 h to 0.24 μm^2 at 36 h; $P < 0.05$; **Fig. 3c–e**). To quantify the growth of individual new PSDs (**Fig. 3b**), we traced PSDs that were first detected at the observation time point $t = 12$ h (**Fig. 3c**). Within 24 h of development at 16 °C, these initially small PSDs reached the average size distribution (**Fig. 3c**). Newly formed PSDs reached half-maximal size (0.12 μm^2) in the first 6 h of observation (age class 0–12 h, **Fig. 3d**). In contrast, 24- to 36-h-old PSDs were only slightly and nonsignificantly smaller than PSDs older than 36 h (0.23 μm^2 to 0.26 μm^2, $P = 0.23$; **Fig. 3d**,**e**). Thus, our assay allowed us to reliably trace individual glutamatergic PSDs only a few hundred nanometers in size over extended time periods *in vivo*. We found that individual glutamatergic PSDs formed distant from existing synapses. These initially very small PSDs then grew until their size finally stabilized (**Fig. 3b**).

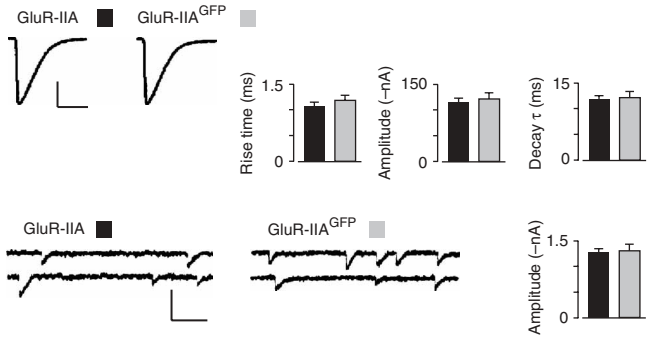

Figure 2 GluR-IIA^{GFP} is fully functional. Spontaneous and nerve-evoked synaptic currents from muscle 6 of *GluRIIA*- and *GluRIIB*-deficient animals rescued with either untagged GluR-IIA or GluR-IIA^{GFP}. Top: representative traces from two-electrode voltage-clamp recordings of both nerve-evoked excitatory junctional currents (scale bars, 50 nA and 20 ms) and mean rise time (10–90%), amplitude and decay time constant τ (80–20%; all ± s.e.m.). Bottom: traces of spontaneous junctional currents (scale bars, 2 nA and 60 ms) and mean amplitude (± s.e.m.). For each genotype, $n = 9$ experiments (Mann Whitney test: $P > 0.1$ for all parameters).

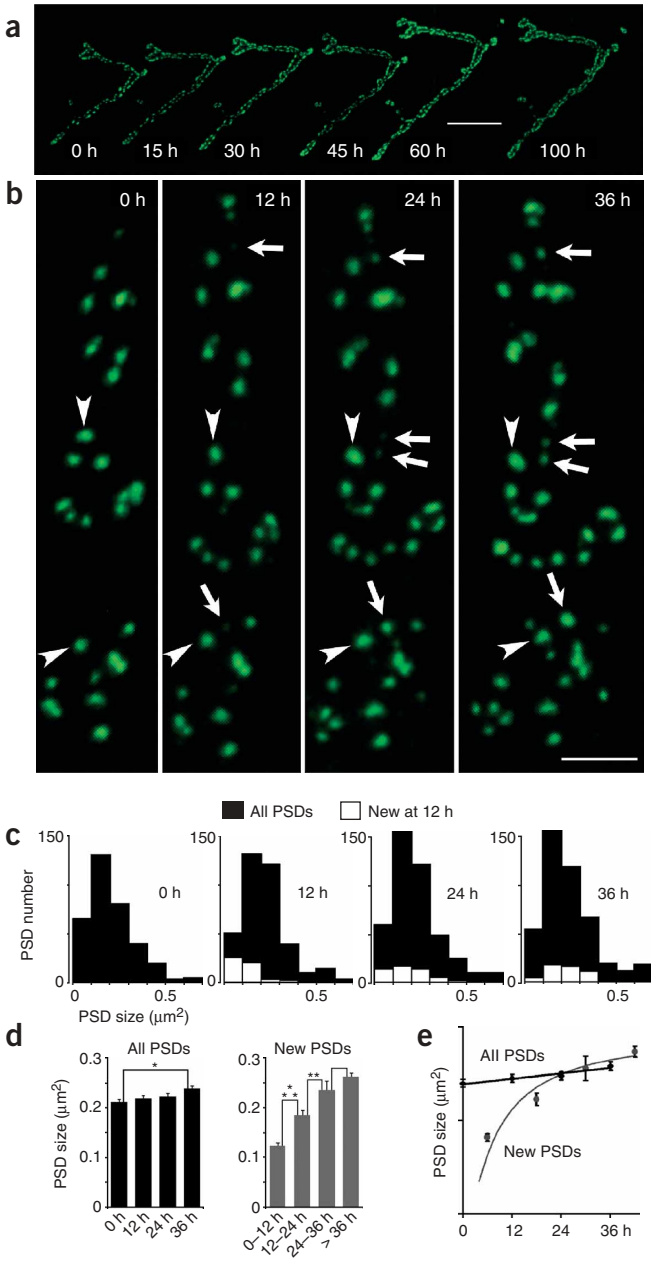

Figure 3 *In vivo* imaging of PSD formation and growth during NMJ development. (**a**,**b**) Confocal *in vivo* imaging of larvae expressing GluR-IIA^{GFP}. The time after the start of the observation is indicated. (**a**) *In vivo* imaging of identified NMJ in lower magnification. Scale bar, 10 μm. (**b**) Identified populations of PSDs shown in higher magnification. Some of the newly appearing PSDs are marked by arrows; some stable PSDs present from the start of observation ($t = 0$ h) are indicated by arrowheads. Scale bar, 4 μm. (**c**) Quantification of PSD dynamics from five pooled imaging series. Histogram plots show the size distribution of PSDs at individual imaging time points by binned PSD sizes (in μm^2). The overall size distributions of PSDs are shown as black bars. PSDs, which were first observed at the 12-h imaging time point, are shown as white bars within black bars. (**d**,**e**) Mean PSD sizes (in μm^2) of the entire population of PSDs are shown as black bars (**d**) and black points (**e**). The mean size of PSDs of a known age (in μm^2) is indicated by gray bars (**d**) and gray points (**e**). In **e** all PSDs older than 36 h are plotted at $t = 42$ h. Error bars: s.e.m.*$P < 0.05$; **$P < 0.015$; ***$P < 0.001$.

Active zones assemble opposite newly forming PSDs

How is the assembly of presynaptic structure and function coordinated with formation of new PSDs? A precondition for the efficient recycling of Ca^{2+} dependent vesicles is the presence of calcium channels in the active zone. Cacophony (Cac) is a voltage-gated calcium channel α1 subunit. When we imaged cacophony labeled with GFP (Cac^{GFP}; ref. 18) *in vivo* together with GluR-IIA^{mRFP} (GluR-IIA labeled with monomeric red fluorescent protein (mRFP)[19]), we found presynaptic calcium channel accumulations tightly associated with postsynaptic GluR-IIA, and vice versa (**Fig. 4a**). To directly visualize presynaptic recycling of synaptic vesicles in relation to PSDs marked with GluR-IIA^{GFP}, internalization of styryl dye FM 5-95 upon high-frequency nerve stimulation[20,21] was visualized on acute preparations of GluR-IIA^{GFP}–positive larvae (**Fig. 4b**). Even the smallest GluR-IIA^{GFP} accumulations were always found in close proximity to presynaptic pools of recycling vesicles (six independent experiments).

To address active zone formation, we used a monoclonal antibody to Drosophila head extracts (Nc82, **Fig. 4c**) that marks the presynaptic zone of individual NMJ synapses opposite the PSD[20,22,23]. The Nc82 antibody recognizes a Drosophila protein showing homology to mammalian CAST (D. Wagh, T.M.R, S.J.S. and E. Buchner, unpublished data). CAST is a presynaptic coiled-coil domain–containing active zone component. In mammals it binds the established active zone marker Bassoon[24–26], for which no Drosophila homolog seems to exist. The *in vivo* imaging of GluR-IIA^{GFP} was then combined with retrospective Nc82 labeling to address the coordination of active zone assembly and PSD formation. The images were taken in either 3-h or 10-h intervals. Subsequently, we fixed the larvae and stained them with antibodies to both GFP and Nc82 (**Fig. 4d**). In mammals, Bassoon has been shown to accumulate at forming glutamatergic synapses before postsynaptic glutamate receptors[27], but we did not detect Nc82 spots without postynaptic GluR-IIA accumulation at the NMJ boutons. In contrast, we frequently found PSDs without Nc82, when the PSDs were maximally 3 h (new formation observed in a 3-h interval) or 10 h old; for PSDs older than 3 h or 10 h, this was very rarely the case (**Fig. 4e**). Our *in vivo* observation of early NMJ synapse formation thus suggested that GluR-IIA–containing glutamate receptors accumulate distant from existing synapses and that a presynaptic active zone invariably differentiates during the growth of these receptor fields. Our data also indicate that postsynaptic accumulation of glutamate receptors can precede the accumulation of some presynaptic active zone components in this system.

The molecular composition of the PSD is dynamic

We next asked how protein dynamics are organized to orchestrate the assembly processes at newly forming and growing synapses. First, we performed FRAP on intact larvae expressing GluR-IIA^{GFP}. When we bleached GluR-IIA^{GFP} from parts of a junction, recovery was very slow, with synaptic signals reappearing only after many hours of development at 25 °C (**Fig. 5a**, compare 3 h to 24 h). To address whether the turnover of postsynaptic proteins is generally low in this synaptic system, a spectrum of postsynaptic proteins shown to influence proper differentiation of postsynaptic structures was subjected to FRAP analysis. First, we produced GFP fusions of cdc42-activated PAK kinase, important for proper glutamate receptor abundance at the NMJ. FRAP of PAK was complete after about 3 h (**Fig. 5b**). Next, GFP-labeled Discs large (Dlg, encoded by *dlg1*) was subjected to FRAP (**Fig. 5c**). Dlg is the founding member of the scaffold-associated PSD-95 protein family, with the DlgA isoform being most similar to PSD-95 itself, and S97-Dlg being similar to SAP-97 (ref. 28). In *dlg1* mutants, PSD size and amount of GluR-IIA per PSD are increased[29,30]. After we

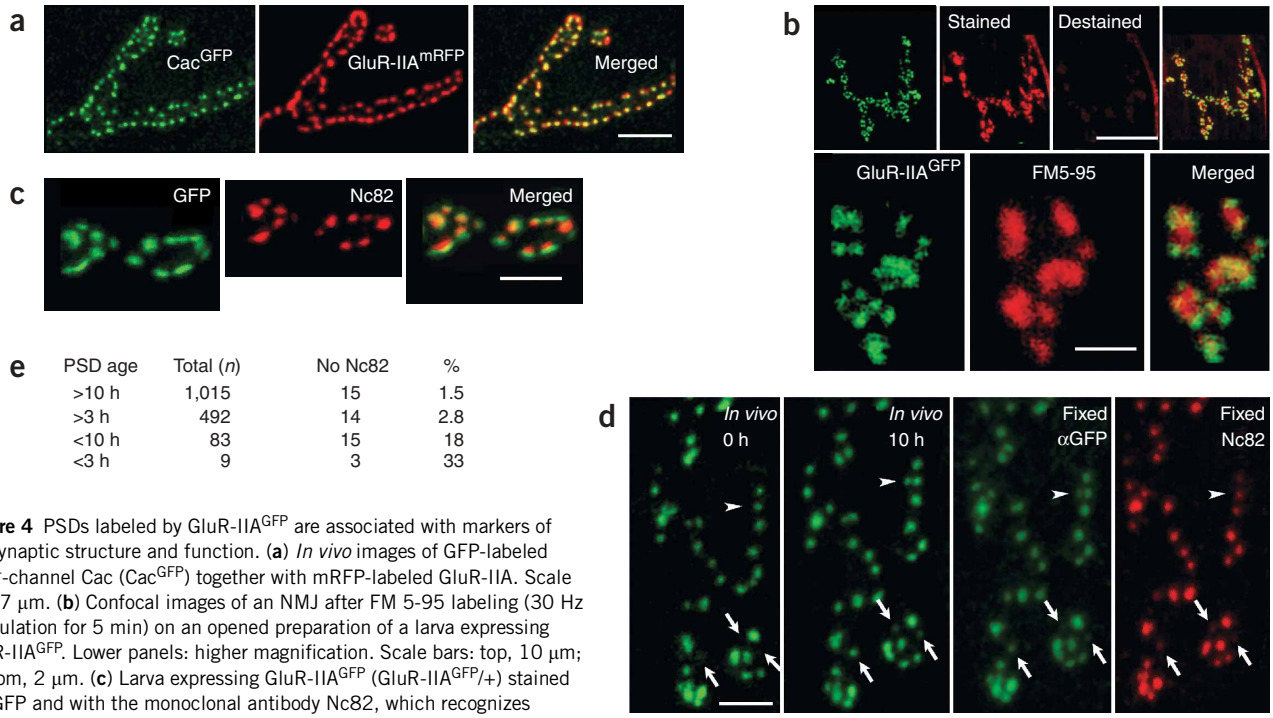

e

PSD age	Total (*n*)	No Nc82	%
>10 h	1,015	15	1.5
>3 h	492	14	2.8
<10 h	83	15	18
<3 h	9	3	33

Figure 4 PSDs labeled by GluR-IIA^{GFP} are associated with markers of presynaptic structure and function. (**a**) *In vivo* images of GFP-labeled Ca^{2+}-channel Cac (Cac^{GFP}) together with mRFP-labeled GluR-IIA. Scale bar, 7 μm. (**b**) Confocal images of an NMJ after FM 5-95 labeling (30 Hz stimulation for 5 min) on an opened preparation of a larva expressing GluR-IIA^{GFP}. Lower panels: higher magnification. Scale bars: top, 10 μm; bottom, 2 μm. (**c**) Larva expressing GluR-IIA^{GFP} (GluR-IIA^{GFP}/+) stained for GFP and with the monoclonal antibody Nc82, which recognizes a presynaptic active zone component. Merged images at bottom. Scale bars, 2 μm. (**d**) Retrospective Nc82 and anti-GFP labeling on a previously *in vivo* imaged larva expressing GluR-IIA^{GFP} (two *in vivo* images taken at a 10-h interval at 25 °C are shown). Although most newly formed receptor fields are associated with Nc82 signal (arrows), some are not (arrowhead). Scale bar, 4 μm. (**e**) Absolute numbers and percentage of receptor fields associated with discernible Nc82 accumulations in larvae subjected to GluR-IIA^{GFP} live imaging followed by retrospective Nc82 and anti-GFP labeling. Newly formed synapses were observed after 3- or 10-h intervals at 25 °C.

bleached parts of the NMJ, the S97-Dlg^{GFP} signal recovered within minutes. It could be argued that membrane protein mobility might be principally slower than that of cytosolic proteins such as Dlg and PAK. Thus, FasII, shown to control NMJ outgrowth and PSD size[29,31], was analyzed on the basis of a functional, on-locus GFP fusion showing wild-type expression level.

Additionally, we used CD8-Shaker^{GFP} (ref. 16) as another example of a postsynaptic transmembrane protein. Here, a CD8 transmembrane domain is targeted to the postsynaptic site of the NMJ by means of its C terminus (derived from the Shaker potassium channel). Although the recovery of CD8-Shaker^{GFP} was still in the range of the cytosolic factors (**Fig. 5d**), FRAP of FasII^{GFP} was slower (**Fig. 5e**). However, recovery of FasII (80% at 10 h) was still much faster than the recovery of GluR-IIA visualized using GluR-IIA^{mRFP} coexpressed with FasII^{GFP} (compare **Fig. 5e**,**f**). FRAP of all postsynaptic proteins apart from GluR-IIA (**Fig. 5a**) occurred at a fast and homogenous rate at the level of individual synapses, whereas GluR-IIA recovery occurred in a very disparate manner, as if restricted to some synapses.

Entry of glutamate receptors correlates with PSD growth

To verify that the recovery of GluR-IIA is indeed restricted to a subset of synapses, we generated larvae expressing both GluR-IIA^{mRFP} and PAK^{GFP}. Twenty-four hours after bleaching both signals, PAK^{GFP} showed complete recovery at all synapses (**Fig. 6a**, left). The recovery of GluR-IIA^{mRFP}, in contrast, was generally weak, although a few synapses in the bleached region had apparently fully recovered (**Fig. 6a**, center and right). Before addressing the reasons for differential recovery of certain synapses, we wanted to exclude that light-induced inactivation of GluR-IIA^{GFP} might alter channel properties and thereby account for its slow FRAP. As mentioned above, *GluRIIA* and *GluRIIB* double mutants are embryonic lethal, but they can be rescued to adult viability by transgenic GluR-IIA^{GFP} expression[8,9]. In such rescued animals all muscle-expressed glutamate receptors should contain GluR-IIA^{GFP} (ref. 11). Here, evoked NMJ currents were indistinguishable before and after completely bleaching their GFP signal (**Fig. 6b**). Thus, GFP bleaching as used during our FRAP experiments did not affect glutamate receptor function. To visualize PSD formation and growth together with GluR-IIA dynamics, larvae expressing both GluR-IIA^{GFP} and GluR-IIA^{mRFP} from genomic transgenes were produced (**Fig. 6c**). After specifically bleaching GluR-IIA^{mRFP}, its recovery allowed the quantification of glutamate receptor entry into the previously bleached PSDs. The GluR-IIA^{GFP} signal thereby served as a reference reflecting the steady-state level of GluR-IIA and PSD organization during synapse formation and growth. Twenty-four hours after bleaching GluR-IIA^{mRFP}, the receptor entry indicated by the recovery of the GluR-IIA^{mRFP} signal was heterogeneous over the PSDs. PSDs that were stable in size during the experiment showed very little or no receptor entry regardless of whether they were large (**Fig. 6c**, white arrowheads) or rather small (**Fig. 6c**, purple arrowhead). Thus, the synaptic population of GluR-IIA is rather immobile once PSDs have reached a stable size.

In contrast, preexisting PSDs that grew during the experiment (**Fig. 6c**, yellow arrowhead) and PSDs that formed *de novo* during the experiment showed considerable glutamate receptor entry (FRAP of GluR-IIA^{mRFP}; **Fig. 6c**, arrows). This suggested that PSD growth is supported by the incorporation of receptors that derive from outside the bleached area and, hence, are not from neighboring synapses. This finding was supported by a quantitative analysis (**Fig. 6d**) showing the ratio of the GluR-IIA^{mRFP} signal relative to the GluR-IIA^{GFP} signal for stable, growing and new synapses (data normalized to the mean value obtained for new synapses). This red/green ratio was highest in new

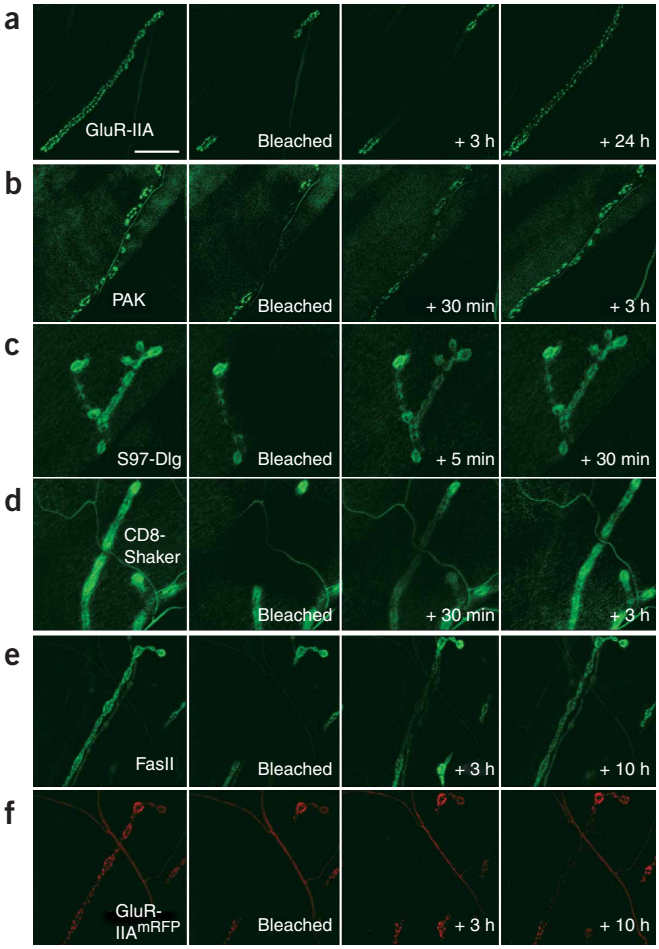

Figure 5 *In vivo* FRAP analysis for several proteins expressed at the postsynaptic site of the NMJ. Shown are confocal images before and directly after bleaching and at later time points. Time after bleaching is indicated. Proteins expressed as GFP fusions and subjected to FRAP analysis are GluR-IIA (**a**), PAK (**b**), Dlg (**c**), CD8-Shaker (**d**), FasII (**e**) and GluR-IIA^{mRFP} (**f**).

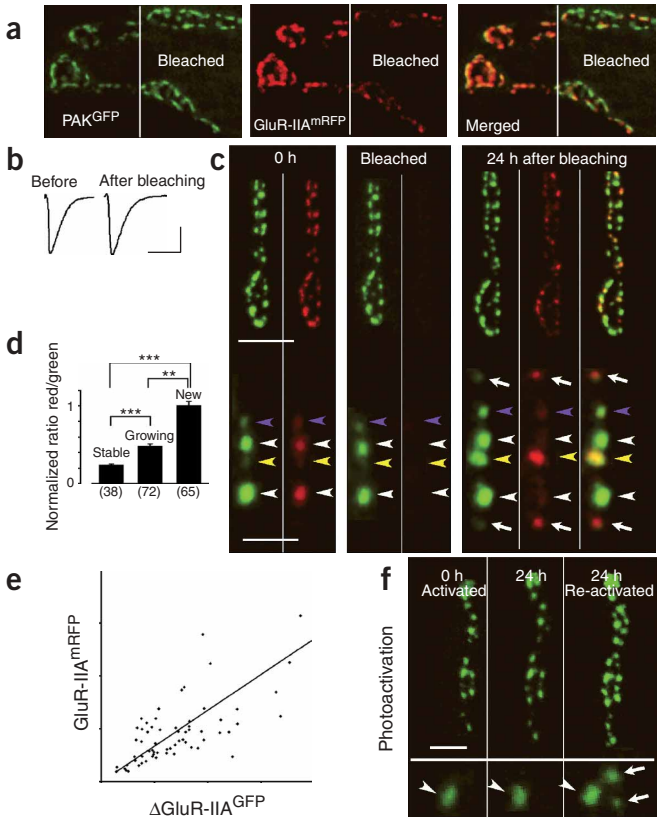

Figure 6 Visualization of glutamate receptor mobility during PSD formation *in vivo*. (**a**) FRAP 24 h after bleaching both signals in parts of the NMJ of larvae expressing both PAK^{GFP} and GluR-IIA^{mRFP}. White line: border of bleach area. (**b**) Evoked junctional currents from *GluRIIA* and *GluRIIB* double-mutant larva expressing GluR-IIA^{GFP}, before and after bleaching GluR-IIA^{GFP}. Scale bars: 50 nA, 20 ms. (**c**) Glutamate receptor entry visualized using FRAP on larvae expressing both GluR-IIA^{GFP} (green) and GluR-IIA^{mRFP} (red). GluR-IIA^{GFP} and GluR-IIA^{mRFP} were imaged before (0 h) and after selectively bleaching GluR-IIA^{mRFP} ('bleached'). Scale bar, 6 μm. Lower half of panels: higher magnification. New (white arrows) and growing (yellow arrowhead) PSDs show higher recovery of GluR-IIA^{mRFP} than stable PSDs (white and purple arrowheads). Scale bar, 2 μm. (**d**) Normalized ratio of GluR-IIA^{mRFP} and GluR-IIA^{GFP} signal 24 h after bleaching. $^{**}P < 0.015$. $^{***}P < 0.001$. Error bars: s.e.m. (**e**) Entry of GluRIIA^{mRFP} at individual PSDs after bleaching versus change in GluRIIA^{GFP} signal (GluRIIA^{GFP}) representing PSD growth over 24 h (arbitrary fluorescence units). R^2 of linear fit is 0.6. (**f**) Confocal time series of a GluR-IIA$^{GFP\text{-}PA}$–expressing junction imaged directly after the first round of photoactivation (left), 24 h after photoactivation (center) and after a subsequent second photoactivation (right). Scale bar, 3 μm. Bottom panels: higher magnification. Arrowhead: a mature or stable PSD; arrows: newly formed PSDs nearby.

synapses, followed by growing and stable synapses. In fact, entry of GluR-IIA (GluR-IIA^{mRFP} after bleach) at newly forming PSDs was directly related to their growth, indicated by the difference of GluR-IIA^{GFP} signal between 24 h and 0 h ($R^2 = 0.60$; **Fig. 6e**).

GluR-IIA is largely immobilized after entry into PSDs

FRAP showed that the preferential entry of extrasynaptic GluR-IIA was directly related to PSD formation and growth. Because large synapses have little GluR-IIA entry but stable receptor field size, the exit of GluR-IIA from mature PSDs should be low. In fact, based on the FRAP data, we calculated that receptor exit from the PSD is below 30% over 24 h at 25 °C. We sought to independently and more directly determine the mobility of PSD-localized GluR-IIA. Thus, we photolabeled glutamate receptors within PSDs and then followed them during synapse formation. For these experiments, we inserted photoactivatable GFP[32] into GluR-IIA (GluR-IIA$^{GFP\text{-}PA}$) and subsequently transgenically expressed it. GFP fluorescence was activated at $t = 0$ h in parts of an NMJ with ultraviolet light (**Fig. 6f**, left). We then imaged the distribution of these photoactivated glutamate receptors 24 h later (**Fig. 6f**, center). PSDs present at the beginning of the experiment kept their labeled glutamate receptors (**Fig. 6f**, central image), independently confirming the FRAP results. Thus, GluR-IIA–containing glutamate receptors seem to be essentially immobilized within the PSDs of NMJ synapses. From the photoactivation data, we calculated GluR-IIA exit from PSDs to be below 20% over 24 h. Moreover, we did not observe any signs of redistribution of photolabeled glutamate receptors into newly forming synapses. Instead, receptors localized within newly formed PSDs became visible only after a second round of photoactivation at the end of the experiment (**Fig. 6f**, right). Hence, FRAP and photoactivation consistently supported the idea that preferential entry of GluR-IIA followed by its immobilization drives PSD growth during synapse formation, whereas PSDs finally stabilize because both entry and exit of GluR-IIA are low.

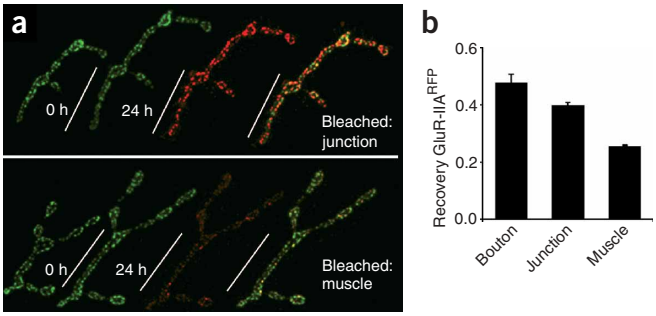

Figure 7 Bleach area–dependence of glutamate receptor FRAP during synapse formation and growth. (**a**) From left to right: GluR-IIA^{GFP} (green) at $t = 0$ h; and GluR-IIA^{GFP} (green), GluR-IIA^{mRFP} (red) and merged signal (yellow) 24 h after bleaching the GluR-IIA^{mRFP} label. Bleaching the entire muscle (bottom) results in low GluR-IIA^{mRFP} recovery at 24 h compared with bleaching the junction (top). (**b**) Quantification of bleach area–dependence of GluR-IIA FRAP. Recovery of the GluR-IIA^{mRFP} signal decreases when the bleached area covers increasing parts of the postsynaptic muscle cell. Recovery was normalized to nonbleached control synapses. Error bars: s.e.m.

Extrasynaptic GluR-IIA selectively enters growing PSDs

We next addressed the origin of the glutamate receptors supporting the growth of newly forming PSDs. We carried out additional FRAP experiments in which the size of the bleached area was systematically varied on consecutive segments of one larva. After we bleached the whole muscle, some GluR-IIA^{mRFP} signal reappeared after 24 h (**Fig. 7a**, bottom), indicating that newly synthesized receptors contribute to PSD growth as previously suggested[33]. When smaller areas were bleached, however, significantly more unbleached GluR-IIA^{mRFP} entered within 24 h compared with bleaching the whole muscle (**Fig. 7a**,**b**). Notably, the position of bleached PSDs relative to the edge of the bleached area had no influence on GluR-IIA FRAP. Thus, potential stores of GluR-IIA close to the synapses did not contribute significantly to PSD growth, which is consistent with the lack of any discernable accumulations of GluR-IIA outside the PSDs. Instead, glutamate receptors are seemingly recruited into newly forming PSDs from pools dispersed over the whole postsynaptic muscle cell.

DISCUSSION

Here we used the Drosophila NMJ to study the formation of a principal glutamatergic synapse *in vivo* and made several key findings.

First, new small glutamatergic PSDs form separately from existing synapses and then grow to a mature size. Mature PSDs are discrete entities that seem to be stable in size and shape over periods of days.

Second, growing receptor fields invariably associate with a presynaptic active zone during further outgrowth. The coordination between pre- and postsynaptic assembly seems to be very tight. In fact, 99.5% of all GluR-IIA spots older than 10 h were associated with active zone markers, and, vice versa, we did not observe any active zone accumulations without GluR-IIA accumulation. In contrast, not all younger GluR-IIA spots were associated with a corresponding active zone. We were somewhat surprised, given the studies on cultured mammalian neurons[34], to find that receptor field/PSD assembly might precede certain aspects of presynaptic active zone assembly and maturation in this system. It will be interesting to address whether glutamatergic synapse types differ in this regard, or whether initial synaptogenesis in culture differs intrinsically from the mode chosen for adding synapses to an already functional circuitry.

Third, new synapses form *de novo*, whereas split-like redistributions of glutamate receptors from existing synapses into new synapses do not seem to contribute to the formation of new synapses. This is important, because splitting events at the glutamatergic PSDs of mammalian CNS synapses have been postulated but are controversial[35–37].

Finally, two complementary strategies for *in vivo* photolabeling of glutamate receptors (FRAP and photoactivation) allowed us to compare glutamate receptor dynamics at growing and stable PSDs. Both approaches showed that GluR-IIA preferentially enters growing PSDs from diffuse extrasynaptic pools. This entry was directly correlated with PSD growth. Once glutamatergic PSDs have reached a certain size, they stabilize, and their glutamate receptor population becomes largely immobilized. In contrast, other postsynaptic transmembrane proteins (for example, FasII) and scaffolding proteins such as the SAP-97/PSD-95 homolog Dlg showed equally high dynamics over all synapses. Previously, genetic experiments showed that more synapses form per NMJ when the level of GluR-IIA expression is increased. Vice versa, the reduction of the GluR-IIA level by one gene dose inhibits the NMJ from producing additional synapses when genetically or behaviorally challenged[33,38,39]. Thus, the entry of glutamate receptors into PSDs (but not the entry of the other postsynaptic proteins investigated) might directly control the growth of the postsynaptic specialization and thereby the growth of synapses. Notably, local translation of GluR-IIA has been suggested to promote activity-dependent synapse formation in this system[33]. On one hand, it will be interesting to further test the role of GluR-IIA as a potential organizer of postsynaptic assembly by combining *in vivo* imaging and functional genetics at the Drosophila NMJ. However, it is well established in the mammalian brain that entry of specific AMPA-type glutamate receptor complexes into preformed synapses can control synapse efficacy over shorter time periods[40,41]. We think it will be interesting to investigate whether glutamate receptor entry can control the formation of mammalian glutamatergic synapses under certain circumstances.

In addressing the origin of receptors integrated into growing synapses, we did not obtain any evidence for internal stores of glutamate receptors. It will thus be interesting to determine the local cues and signals at PSDs that specifically control GluR-IIA entry and immobilization during PSD growth. We suspect that GluR-IIA populations residing in the extrasynaptic muscle plasma membrane support PSD growth. Electrophysiology has, in fact, demonstrated the existence of glutamate receptors in the extrasynaptic membrane of Drosophila muscles[17]. Such receptors might diffuse laterally in the membrane partitioning in and out of synapses, where they likely have a low residence time[42,43]. This pool of unbound receptors might be fundamentally different from a second pool of receptors, which is 'trapped' in PSDs, as demonstrated recently by tracking individual glutamate receptor complexes in cultured mammalian neurons[42].

During the few days of larval development, the synaptic current per Drosophila NMJ increases by nearly two orders of magnitude to keep pace with the growing postsynaptic muscle cell[17,39]. Our data imply that GluRIIA–containing glutamate receptors seem to become particularly 'invested' into the formation and subsequent outgrowth of new synapses, but less so in the enlargement of preexisting synapses. At average NMJ synapses, it is likely that glutamate receptors are not saturated for glutamate during vesicle exocytosis[44,45]. We speculate that at small, newly forming synapses, a higher proportion of glutamate receptors might be activated during glutamate release because of the smaller physical distance from the exact position of the presynaptic release site. To achieve an increase in the overall NMJ current, it therefore might be more efficient to insert new receptors into these small synapses than to insert them into the large receptor fields of

mature size synapses, which are unlikely to be saturated upon presynaptic stimulation. Thereby, the 'drive' of the Drosophila NMJ toward increasing overall transmission strength might be the deeper reason behind strongly stabilizing receptors once they are integrated.

Examining the dynamic molecular composition of glutamatergic synapses in more detail by further applying both *in vivo* imaging and the powerful genetics of Drosophila should help clarify principal rules for assembly and remodeling of glutamatergic synapses. Notably, at the Drosophila NMJ, activity-dependent formation of additional synapses has been described on the basis of experience-dependent and genetically evoked processes[39,46,47].

METHODS

Molecular biology and genetics. To express fluorescently tagged GluR-IIA, we used an *Eco*RI/*Xba*I genomic fragment from BACR35L07 entailing a 1.2-kb sequence upstream of start codon. Fluorescent tags (GFP, mRFP and photoactivatable GFP) were inserted in the intracellular C terminus of GluR-IIA after Ser893. GluR-IIA^{GFP} and GluR-IIA were tested for rescue activity in the *GluRIIA* and *GluRIIB* double mutant (*Df(2L)cl*^{h4} *GluRIIA*^{SP22} *GluRIIB*^{SP22}) background[9]. All GluR-IIA constructs produced rescued larvae in a mendelian ratio. For *in vivo* imaging, all GluR-IIA constructs were expressed in a background heterozygous for the *GluRIIA* null allele. To construct PAK^{GFP}, the Myc tag in UAS-Pak-myc[48] was replaced by EGFP. Transgenic PAK^{GFP} expression was induced at 16 °C using G14-Gal4 (ref. 49). CD8-Shaker^{GFP} is a direct fusion with the Mhc promotor[16]. UAS-S97-Dlg^{GFP} (ref. 28) expression was induced with C57-Gal4. FasII^{GFP} used in FRAP experiments is an insertion of a GFP into the last intron of the X-chromosomal *fasII* locus identified in a joined screening effort (SPP1111 Cell Polarity) using exon-trap screening[50]. More details concerning the cloning of these constructs are available on request.

Electrophysiology and FM 5-95 labeling. Intracellular TEVC recordings were made at 22 °C from muscle fiber 6 of abdominal segments 2 and 3 from late third instar male larvae as described[11]. FM 5-95 uptake was done essentially as described[21]. Briefly, terminals at muscle 4 were labeled by replacing normal saline with normal saline containing 20 μM FM 5-95 (T-23360, Molecular Probes) followed by stimulating the innervating nerve at 30 Hz for 5 min. After stimulation, preparations were washed three times with Ca^{2+}-free saline. Destaining was done by applying high-K^+ saline for 5 min.

Antibodies. Antibodies were used at the following concentrations: mouse antibody Nc82, 1:100 (gift of E. Buchner, University of Würzburg, Germany); rabbit antibody to PAK, 1:2,000 (gift of N. Harden, Simon Fraser University, Burnaby, Canada); mouse antibody to FasII, 1:50 (Developmental Studies Hybridoma Bank); rabbit antibody to GFP, 1:500 (Molecular Probes); mouse antibody to GluR-IIA, 1:100 (Developmental Studies Hybridoma Bank); and rabbit antibody to GluR-IIC[11], 1:500.

Anesthetization of Drosophila larvae. Because nonanesthetized Drosophila larvae move considerably, *in vivo* imaging on the level of individual synapses demands stable anesthetization to allow confocal imaging.

The application of 15% (v/v) of Desflurane (Baxter) for 2 min proved ideal because onset and recovery from anesthetization were fast, with anesthetized larvae being immobile and no longer showing internal movements. Second or third instar larvae were mounted in a custom-made imaging chamber, which was connected to a two-channel respiration system. Control experiments using ten consecutive anesthetizations, separated by 5-min recovery intervals, showed neither developmental delay nor increased mortality in anesthetized larvae compared with nonanesthetized but otherwise identically treated sibling larvae.

Image acquisition. *In vivo* images were taken of NMJs on muscle 27, located shortly beneath the larval cuticle. *In vivo* imaging was performed on a Leica DM IRE2 microscope equipped with a Leica TCS SP2 AOBS scanhead. FM 5-95 labels were scanned on a Leica DM LFSA equipped with a Leica TCS SP2 scanhead (Leica Microsystems). The time series shown in **Figure 3** was carried out at 16 °C; all other experiments were performed at 25 °C. The image processing analysis was performed using ImageJ 1.32b (US National Institutes of Health; http://rsb.info.nih.gov/ij/download.html). Further details on imaging and data processing are available on request.

ACKNOWLEDGMENTS

We thank H. Jäckle, G. Stuart and J. Eilers for comments on the manuscript; A. Schönle, J. Rietdorf, S. Höning and D. Sandstrom for advice; H. Aberle, U. Thomas, R. Ordway, E. Buchner, N. Harding, A. DiAntonio and R. Tsien for fly stocks and reagents; M. Richter for technical assistance and the screening team of Deutsche Forschungsgemeinschaft (DFG) SPP1111 Cell Polarity. This work was supported by grants from the DFG to S.J.S. and M.H.

COMPETING INTERESTS STATEMENT

The authors declare that they have no competing financial interests.

Received 17 March; accepted 23 May 2005
Published online at http://www.nature.com/natureneuroscience/

1. Chklovskii, D.B., Mel, B.W. & Svoboda, K. Cortical rewiring and information storage. *Nature* **431**, 782–788 (2004).
2. Gundelfinger, E.D., Kessels, M.M. & Qualmann, B. Temporal and spatial coordination of exocytosis and endocytosis. *Nat. Rev. Mol. Cell Biol.* **4**, 127–139 (2003).
3. Washbourne, P., Bennett, J.E. & McAllister, A.K. Rapid recruitment of NMDA receptor transport packets to nascent synapses. *Nat. Neurosci.* **5**, 751–759 (2002).
4. Bresler, T. *et al.* Postsynaptic density assembly is fundamentally different from presynaptic active zone assembly. *J. Neurosci.* **24**, 1507–1520 (2004).
5. Niell, C.M. & Smith, S.J. Live optical imaging of nervous system development. *Annu. Rev. Physiol.* **66**, 771–798 (2004).
6. Featherstone, D.E. & Broadie, K. Surprises from *Drosophila*: genetic mechanisms of synaptic development and plasticity. *Brain Res. Bull.* **53**, 501–511 (2000).
7. Gramates, L.S. & Budnik, V. Assembly and maturation of the *Drosophila* larval neuromuscular junction. *Int. Rev. Neurobiol.* **43**, 93–117 (1999).
8. Petersen, S.A., Fetter, R.D., Noordermeer, J.N., Goodman, C.S. & DiAntonio, A. Genetic analysis of glutamate receptors in *Drosophila* reveals a retrograde signal regulating presynaptic transmitter release. *Neuron* **19**, 1237–1248 (1997).
9. DiAntonio, A., Petersen, S.A., Heckmann, M. & Goodman, C.S. Glutamate receptor expression regulates quantal size and quantal content at the *Drosophila* neuromuscular junction. *J. Neurosci.* **19**, 3023–3032 (1999).
10. Marrus, S.B., Portman, S.L., Allen, M.J., Moffat, K.G. & DiAntonio, A. Differential localization of glutamate receptor subunits at the *Drosophila* neuromuscular junction. *J. Neurosci.* **24**, 1406–1415 (2004).
11. Qin, G. *et al.* Four different subunits are essential for expressing the synaptic glutamate receptor at neuromuscular junctions of *Drosophila*. *J. Neurosci.* **25**, 3209–3218 (2005).
12. Schuster, C.M., Davis, G.W., Fetter, R.D. & Goodman, C.S. Genetic dissection of structural and functional components of synaptic plasticity. I. Fasciclin II controls synaptic stabilization and growth. *Neuron* **17**, 641–654 (1996).
13. Schuster, C.M. *et al.* Molecular cloning of an invertebrate glutamate receptor subunit expressed in *Drosophila* muscle. *Science* **254**, 112–114 (1991).
14. Albin, S.D. & Davis, G.W. Coordinating structural and functional synapse development: postsynaptic p21-activated kinase independently specifies glutamate receptor abundance and postsynaptic morphology. *J. Neurosci.* **24**, 6871–6879 (2004).
15. Sone, M. *et al.* Synaptic development is controlled in the periactive zones of *Drosophila* synapses. *Development* **127**, 4157–4168 (2000).
16. Zito, K., Parnas, D., Fetter, R.D., Isacoff, E.Y. & Goodman, C.S. Watching a synapse grow: noninvasive confocal imaging of synaptic growth in *Drosophila*. *Neuron* **22**, 719–729 (1999).
17. Broadie, K. & Bate, M. Activity-dependent development of the neuromuscular synapse during *Drosophila* embryogenesis. *Neuron* **11**, 607–619 (1993).
18. Kawasaki, F., Zou, B., Xu, X. & Ordway, R.W. Active zone localization of presynaptic calcium channels encoded by the cacophony locus of *Drosophila*. *J. Neurosci.* **24**, 282–285 (2004).
19. Campbell, R.E. *et al.* A monomeric red fluorescent protein. *Proc. Natl. Acad. Sci. USA* **99**, 7877–7882 (2002).
20. Wucherpfennig, T., Wilsch-Brauninger, M. & Gonzalez-Gaitan, M. Role of *Drosophila* Rab5 during endosomal trafficking at the synapse and evoked neurotransmitter release. *J. Cell Biol.* **161**, 609–624 (2003).
21. Kuromi, H. & Kidokoro, Y. Selective replenishment of two vesicle pools depends on the source of Ca2+ at the *Drosophila* synapse. *Neuron* **35**, 333–343 (2002).
22. Heimbeck, G., Bugnon, V., Gendre, N., Haberlin, C. & Stocker, R.F. Smell and taste perception in *Drosophila melanogaster* larva: toxin expression studies in chemosensory neurons. *J. Neurosci.* **19**, 6599–6609 (1999).
23. Marrus, S.B. & DiAntonio, A. Preferential localization of glutamate receptors opposite sites of high presynaptic release. *Curr. Biol.* **14**, 924–931 (2004).
24. Takao-Rikitsu, E. *et al.* Physical and functional interaction of the active zone proteins, CAST, RIM1, and Bassoon, in neurotransmitter release. *J. Cell Biol.* **164**, 301–311 (2004).
25. Ohtsuka, T. *et al.* Cast: a novel protein of the cytomatrix at the active zone of synapses that forms a ternary complex with RIM1 and munc13–1. *J. Cell Biol.* **158**, 577–590 (2002).
26. Wang, Y., Liu, X., Biederer, T. & Sudhof, T.C. A family of RIM-binding proteins regulated by alternative splicing: Implications for the genesis of synaptic active zones. *Proc. Natl. Acad. Sci. USA* **99**, 14464–14469 (2002).

27. Shapira, M. *et al.* Unitary assembly of presynaptic active zones from Piccolo-Bassoon transport vesicles. *Neuron* **38**, 237–252 (2003).
28. Bachmann, A. *et al.* Cell type-specific recruitment of *Drosophila* Lin-7 to distinct MAGUK-based protein complexes defines novel roles for Sdt and Dlg-S97. *J. Cell Sci.* **117**, 1899–1909 (2004).
29. Stewart, B.A., Schuster, C.M., Goodman, C.S. & Atwood, H.L. Homeostasis of synaptic transmission in *Drosophila* with genetically altered nerve terminal morphology. *J. Neurosci.* **16**, 3877–3886 (1996).
30. Chen, K. & Featherstone, D.E. Discs-large (DLG) is clustered by presynaptic innervation and regulates postsynaptic glutamate receptor subunit composition in *Drosophila*. *BMC Biol.* **3**, 1 (2005).
31. Schuster, C.M., Davis, G.W., Fetter, R.D. & Goodman, C.S. Genetic dissection of structural and functional components of synaptic plasticity. II. Fasciclin II controls presynaptic structural plasticity. *Neuron* **17**, 655–667 (1996).
32. Patterson, G.H. & Lippincott-Schwartz, J. A photoactivatable GFP for selective photolabeling of proteins and cells. *Science* **297**, 1873–1877 (2002).
33. Sigrist, S.J. *et al.* Postsynaptic translation affects the efficacy and morphology of neuromuscular junctions. *Nature* **405**, 1062–1065 (2000).
34. Ziv, N.E. & Garner, C.C. Principles of glutamatergic synapse formation: seeing the forest for the trees. *Curr. Opin. Neurobiol.* **11**, 536–543 (2001).
35. Toni, N., Buchs, P.A., Nikonenko, I., Bron, C.R. & Muller, D. LTP promotes formation of multiple spine synapses between a single axon terminal and a dendrite. *Nature* **402**, 421–425 (1999).
36. Fiala, J.C., Allwardt, B. & Harris, K.M. Dendritic spines do not split during hippocampal LTP or maturation. *Nat. Neurosci.* **5**, 297–298 (2002).
37. Toni, N. *et al.* Remodeling of synaptic membranes after induction of long-term potentiation. *J. Neurosci.* **21**, 6245–6251 (2001).
38. Sigrist, S.J., Thiel, P.R., Reiff, D.F. & Schuster, C.M. The postsynaptic glutamate receptor subunit DGluR-IIA mediates long-term plasticity in *Drosophila*. *J. Neurosci.* **22**, 7362–7372 (2002).
39. Sigrist, S.J., Reiff, D.F., Thiel, P.R., Steinert, J.R. & Schuster, C.M. Experience-dependent strengthening of *Drosophila* neuromuscular junctions. *J. Neurosci.* **23**, 6546–6556 (2003).
40. Shi, S., Hayashi, Y., Esteban, J.A. & Malinow, R. Subunit-specific rules governing AMPA receptor trafficking to synapses in hippocampal pyramidal neurons. *Cell* **105**, 331–343 (2001).
41. Malinow, R. & Malenka, R.C. AMPA receptor trafficking and synaptic plasticity. *Annu. Rev. Neurosci.* **25**, 103–126 (2002).
42. Borgdorff, A.J. & Choquet, D. Regulation of AMPA receptor lateral movements. *Nature* **417**, 649–653 (2002).
43. Tardin, C., Cognet, L., Bats, C., Lounis, B. & Choquet, D. Direct imaging of lateral movements of AMPA receptors inside synapses. *EMBO J.* **22**, 4656–4665 (2003).
44. Karunanithi, S., Marin, L., Wong, K. & Atwood, H.L. Quantal size and variation determined by vesicle size in normal and mutant *Drosophila* glutamatergic synapses. *J. Neurosci.* **22**, 10267–10276 (2002).
45. Daniels, R.W. *et al.* Increased expression of the *Drosophila* vesicular glutamate transporter leads to excess glutamate release and a compensatory decrease in quantal content. *J. Neurosci.* **24**, 10466–10474 (2004).
46. Budnik, V., Zhong, Y. & Wu, C.F. Morphological plasticity of motor axons in *Drosophila* mutants with altered excitability. *J. Neurosci.* **10**, 3754–3768 (1990).
47. Renger, J.J., Ueda, A., Atwood, H.L., Govind, C.K. & Wu, C.F. Role of cAMP cascade in synaptic stability and plasticity: ultrastructural and physiological analyses of individual synaptic boutons in *Drosophila* memory mutants. *J. Neurosci.* **20**, 3980–3992 (2000).
48. Ang, L.H., Kim, J., Stepensky, V. & Hing, H. Dock and Pak regulate olfactory axon pathfinding in *Drosophila*. *Development* **130**, 1307–1316 (2003).
49. Aberle, H. *et al.* Wishful thinking encodes a BMP type II receptor that regulates synaptic growth in *Drosophila*. *Neuron* **33**, 545–558 (2002).
50. Morin, X., Daneman, R., Zavortink, M. & Chia, W. A protein trap strategy to detect GFP-tagged proteins expressed from their endogenous loci in *Drosophila*. *Proc. Natl. Acad. Sci. USA* **98**, 15050–15055 (2001).